An analytic solution of projectile motion with the quadratic resistance law using the homotopy analysis method

Kazuki Yabushita[1], Mariko Yamashita[2] and Kazuhiro Tsuboi[3]

[1] Department of Mechanical Systems Engineering, National Defense Academy,
1-10-20 Hashirimizu, Yokosuka, Kanagawa 239-8686, Japan
[2] Graduate School of Science and Engineering, National Defense Academy,
1-10-20 Hashirimizu, Yokosuka, Kanagawa 239-8686, Japan
[3] Department Intelligent System Engineering, IBARAKI University, 4-12-1 Naka-narusawa,
Hitachi, Ibaraki 316-8511, Japan

E-mail: yabu@nda.ac.jp

Abstract

We consider the problem of two-dimensional projectile motion in which the resistance acting on an object moving in air is proportional to the square of the velocity of the object (quadratic resistance law). It is well known that the quadratic resistance law is valid in the range of the Reynolds number: $1 \times 10^3 \sim 2 \times 10^5$ (for instance, a sphere) for practical situations, such as throwing a ball. It has been considered that the equations of motion of this case are unsolvable for a general projectile angle, although some solutions have been obtained for a small projectile angle using perturbation techniques. To obtain a general analytic solution, we apply Liao's homotopy analysis method to this problem. The homotopy analysis method, which is different from a perturbation technique, can be applied to a problem which does not include small parameters. We apply the homotopy analysis method for not only governing differential equations, but also an algebraic equation of a velocity vector to extend the radius of convergence. Ultimately, we obtain the analytic solution to this problem and investigate the validation of the solution.

PACS numbers: 01.55.+b, 02.30.Hq, 04.25.−g

1. Introduction

The projectile motion problem with air resistance is considered in this paper. According to fluid dynamics [1], linear air resistance law (the air resistance is proportional to the magnitude of velocity) and quadratic resistance law (the air resistance is proportional to the square of the

magnitude of velocity) are known as resistance laws of a moving object in air. It is known that a small sphere moving slowly, such as a particle of mist, has linear air resistance. The motion equation of this case is solvable analytically. This state is indicated by $Re < 1$. Re is the non-dimensional parameter called the Reynolds number, and is defined as $Re = UD/\nu$, where U is a velocity of the object, D is a diameter in case the object is a sphere and ν is the coefficient of kinematic viscosity of the air (1.5×10^{-5} m^2 s^{-1}). Quadratic air resistance acts on a sphere for practical situations such as throwing a ball in $1 \times 10^3 < Re < 2 \times 10^5$. The motion equation of this case is unsolvable analytically, although the problem is fundamental and practical in elementary dynamics. Most objects, including a sphere, have a quadratic air resistance in their own Reynolds number ranges. The motion equation of this case is

$$M\hat{v}'(\hat{t}) = -\frac{1}{2}\rho|\hat{v}(\hat{t})|^2 AC_D\frac{\hat{v}(\hat{t})}{|\hat{v}(\hat{t})|} + K, \tag{1}$$

where M is the mass of the object, ρ is the air density, A is the projected area of the object ($A = \pi a^2$ when a sphere's radius is a), $\hat{v}$ is the velocity of the object, $K = (0, -Mg)$ is the gravitational force vector, g is the acceleration of gravity and C_D is the drag coefficient (C_D is considered constant in the range of $1 \times 10^3 < Re < 2 \times 10^5$). Equation (1) can be written using the components of a velocity vector, $\hat{v} = (\hat{u}, \hat{v})$ as follows:

$$\hat{u}'(\hat{t}) + \alpha\sqrt{\hat{u}(\hat{t})^2 + \hat{v}(\hat{t})^2}\hat{u}(\hat{t}) = 0, \tag{2}$$

$$\hat{v}'(\hat{t}) + \alpha\sqrt{\hat{u}(\hat{t})^2 + \hat{v}(\hat{t})^2}\hat{v}(\hat{t}) + g = 0, \tag{3}$$

$$\alpha = \frac{\rho\pi a^2 C_D}{2M}. \tag{4}$$

The analytic solutions of falling motion problems with linear air resistance and with quadratic air resistance have already been obtained. Also, the case of projectile motion with linear air resistance has already been solved. As mentioned before, the case of projectile motion with quadratic air resistance has previously been unsolvable without adding some specific conditions.

We mention several analytic solutions obtained in the past and their conditions.

Firstly, Lamb described in his book [2] that this problem is solvable approximately under the condition $\hat{u} \gg \hat{v}$ (nearly horizontal path). The solution is

$$\hat{y}(\hat{x}) = \left(\frac{\hat{V}_0}{\hat{U}_0} + \frac{1}{2}\frac{g}{\alpha\hat{U}_0^2}\right)\hat{x} - \frac{1}{4}\frac{g}{\alpha^2\hat{U}_0^2}(e^{2\alpha\hat{x}} - 1), \tag{5}$$

where $\hat{U}_0$ is the horizontal initial velocity and $\hat{V}_0$ is the perpendicular initial velocity. However, this solution is unavailable in that the order of $\hat{v}$ is the same as the order of $\hat{u}$.

Secondly, Parker [3] solved this problem and obtained approximate solutions for both short and long times. However, Parker's short-time approximate solution is the same as Lamb's solution. Hence, this solution is only available for a nearly horizontal path. His long-time approximate solution can be connected to the present solution which we obtain in this paper.

Thirdly, Tsuboi [4] applied perturbation techniques to this problem under the conditions of $\alpha \ll 1$ and $\hat{U}_0 \gg \hat{V}_0$ (nearly horizontal path). As a result, the first-order approximate solution was obtained:

$$\hat{x}(\hat{t}) = \hat{U}_0\hat{t} + \frac{\alpha\hat{t}^2}{24}\left[-(g\hat{t})^2 + 4\hat{V}_0 g\hat{t} - 6(2\hat{U}_0^2 + \hat{V}_0^2)\right], \tag{6}$$

$$\hat{y}(\hat{t}) = \hat{V}_0\hat{t} - \frac{g\hat{t}^2}{2} + \frac{\alpha\hat{t}^2}{120\hat{U}_0}\big[3(g\hat{t})^3 - 15\hat{V}_0(g\hat{t})^2 + \big(20\hat{U}_0^2 + 30\hat{V}_0^2\big)g\hat{t} - 30\hat{V}_0\big(2\hat{U}_0^2 + \hat{V}_0^2\big)\big].$$
(7)

Finally, the hodograph equation [5, 6], the relationship between the velocity $\hat{f} = \sqrt{\hat{u}^2 + \hat{v}^2}$ at the certain point in the orbit and the angle $\theta = \tan^{-1}\hat{v}/\hat{u}$ can be derived under the quadratic air resistance law as follows:

$$\frac{1}{\hat{f}^2(\theta)} = \cos^2\theta\left(C - \frac{\alpha}{g}\tanh^{-1}(\sin\theta)\right) - \frac{\alpha}{g}\sin\theta,$$
(8)

where

$$C = \frac{1}{\cos^2\theta_0}\left(\hat{f}_0^{-2} + \frac{\alpha}{g}\cos^2\theta_0\tanh^{-1}(\sin\theta_0) + \frac{\alpha}{g}\sin\theta_0\right),$$
(9)

$$\hat{f}_0 = \sqrt{\hat{U}_0^2 + \hat{V}_0^2},$$
(10)

$$\theta_0 = \tan^{-1}\frac{\hat{V}_0}{\hat{U}_0}.$$
(11)

The position $(\hat{x}, \hat{y})$ and the time $\hat{t}$ are described using $\hat{f}(\theta)$ and θ as follows:

$$\hat{x}(\theta) = -\frac{1}{g}\int_{\theta_0}^{\theta}\{\hat{f}(\theta)\}^2\,\mathrm{d}\theta,$$
(12)

$$\hat{y}(\theta) = -\frac{1}{g}\int_{\theta_0}^{\theta}\tan\theta\{\hat{f}(\theta)\}^2\,\mathrm{d}\theta,$$
(13)

$$\hat{t}(\theta) = -\frac{1}{g}\int_{\theta_0}^{\theta}\sec\theta\,\hat{f}(\theta)\,\mathrm{d}\theta.$$
(14)

However, the above equations cannot be integrated without numerical techniques. This means that it is impossible to obtain the orbit analytically.

The perturbation technique has frequently been used to solve nonlinear problems. However, the perturbation technique can only be used to solve problems including small parameters.

The homotopy analysis method [7] is a new analytic method introduced by Liao in 1992 to solve nonlinear problems. As opposed to the perturbation technique, the homotopy analysis method can be applied to problems that do not include small parameters. It is also shown [7, 8] that the Adomian decomposition method is a special case of the homotopy analysis method. Liao solved various nonlinear problems using the homotopy analysis method and in 1992 obtained a second-order analytic solution of a simple pendulum that was in agreement with the numerical result [9]. In 1997 Liao solved the governing equation of a two-dimensional viscous laminar flow past a semi-infinite flat plate [10]. The inner and outer solutions had already been obtained using the perturbation technique. The inner solution was extended to the outer region of the boundary layer using the homotopy analysis method. It was found that Liao's solution was valid in the whole region of the boundary layer. Also, extended solutions of the unsteady boundary layer flows were derived by Liao et al [11, 12]. In 2002 Liao obtained the approximate solution of the drag coefficient for viscous flow past a sphere by solving the Navier–Stokes equation in the range of $Re < 30$ [13].

In this paper, we apply Liao's homotopy analysis method to the problem of projectile motion with quadratic air resistance for an arbitrary angle of projection. We obtain an analytic solution expressed as power series for this problem.

2. The governing equations

The governing equations (2), (3) of projectile motion with quadratic air resistance can be expressed in the non-dimensional form as follows:

$$\frac{du(t)}{dt} + f(t)u(t) = 0, \tag{15}$$

$$\frac{dv(t)}{dt} + f(t)v(t) + 1 = 0, \tag{16}$$

where

$$u(t) = \frac{\hat{u}(\hat{t})}{v_t} = \hat{u}(\hat{t})\sqrt{\frac{\alpha}{g}}, \tag{17}$$

$$v(t) = \frac{\hat{v}(\hat{t})}{v_t} = \hat{v}(\hat{t})\sqrt{\frac{\alpha}{g}}, \tag{18}$$

$$t = \frac{\hat{t}}{v_t/g} = \hat{t}\sqrt{\alpha g}, \tag{19}$$

$$f(t) = \sqrt{u^2(t) + v^2(t)}, \tag{20}$$

$$v_t = \sqrt{\frac{g}{\alpha}}. \tag{21}$$

The velocity v_t is called terminal velocity. Initial conditions are

$$u(0) = \frac{\hat{U}_0}{v_t} = U_0, \qquad v(0) = \frac{\hat{V}_0}{v_t} = V_0. \tag{22}$$

3. The homotopy analysis solution

We construct the zeroth-order deformation equations in the first step of analysis. At first, we tried a standard method in which the homotopy analysis method is used only for governing differential equations (15) and (16), however, the obtained solution had diverged near the top of the orbit. Therefore, we construct the zeroth-order deformation equations for not only (15) and (16), but for also (20) as follows:

$$(1-p)\frac{\partial U(t; p, \hbar_1, \hbar_2)}{\partial t}$$
$$+ p\hbar_1\left[\frac{\partial U(t; p, \hbar_1, \hbar_2)}{\partial t} + F(t; p, \hbar_1, \hbar_2)U(t; p, \hbar_1, \hbar_2)\right] = 0, \tag{23}$$

$$(1-p)\frac{\partial V(t; p, \hbar_1, \hbar_2)}{\partial t}$$
$$+ p\hbar_1\left[\frac{\partial V(t; p, \hbar_1, \hbar_2)}{\partial t} + F(t; p, \hbar_1, \hbar_2)V(t; p, \hbar_1, \hbar_2) + 1\right] = 0, \tag{24}$$

$$(1-p)\left[F^2(t; p, \hbar_1, \hbar_2) - U_0^2 - V_0^2\right]$$
$$+ p\hbar_2[F^2(t; p, \hbar_1, \hbar_2) - U^2(t; p, \hbar_1, \hbar_2) - V^2(t; p, \hbar_1, \hbar_2)] = 0, \tag{25}$$

$$U(0; p, \hbar_1, \hbar_2) = U_0, \qquad V(0; p, \hbar_1, \hbar_2) = V_0, \tag{26}$$

where p is the embedding parameter and $\hbar_1, \hbar_2$ are the homotopy parameters which are non-zero real numbers. When the embedding parameter $p = 0$, (23)–(25) are transformed into the linear differential equations $\partial U(t; 0, \hbar_1, \hbar_2)/\partial t = 0$, $\partial V(t; 0, \hbar_1, \hbar_2)/\partial t = 0$

and $F(t; 0, \hbar_1, \hbar_2) = \sqrt{U_0^2 + V_0^2}$. These equations must not have physical meaning in the homotopy analysis method, however, it is necessary that those equations are solved analytically. When the embedding parameter $p = 1$, (23)–(25) are transformed into the nonlinear differential equations that are the same as (15), (16) and (20), which are the governing equations for this system. That is to say, $u(t) = U(t; 1, \hbar_1, \hbar_2)$, $v(t) = V(t; 1, \hbar_1, \hbar_2)$ and $f(t) = F(t; 1, \hbar_1, \hbar_2)$. The solutions $U(t; 0, \hbar_1, \hbar_2)$, $V(t; 0, \hbar_1, \hbar_2)$ and $F(t; 0, \hbar_1, \hbar_2)$ are connected to the solutions $U(t; 1, \hbar_1, \hbar_2)$, $V(t; 1, \hbar_1, \hbar_2)$ and $F(t; 1, \hbar_1, \hbar_2)$ by Taylor's expansion. Namely, $U(t; p, \hbar_1, \hbar_2)$, $V(t; p, \hbar_1, \hbar_2)$ and $F(t; p, \hbar_1, \hbar_2)$ are homotopies between $U(t; 0, \hbar_1, \hbar_2)$, $V(t; 0, \hbar_1, \hbar_2)$, $F(t; 0, \hbar_1, \hbar_2)$ and $U(t; 1, \hbar_1, \hbar_2)$, $V(t; 1, \hbar_1, \hbar_2)$, $F(t; 1, \hbar_1, \hbar_2)$. Homotopy parameters $\hbar_1, \hbar_2$ affect the convergence of the solution. According to Liao's paper, the convergence region of the solution seems to increase as $\hbar_1, \hbar_2$ approach zero.

Expanding $U(t; p, \hbar_1, \hbar_2)$, $V(t; p, \hbar_1, \hbar_2)$ and $F(t; p, \hbar_1, \hbar_2)$ to Taylor's series at $p = 0$, we have

$$U(t; p, \hbar_1, \hbar_2) = \sum_{m=0}^{+\infty} u_m(t; \hbar_1, \hbar_2) p^m, \tag{27}$$

$$V(t; p, \hbar_1, \hbar_2) = \sum_{m=0}^{+\infty} v_m(t; \hbar_1, \hbar_2) p^m, \tag{28}$$

$$F(t; p, \hbar_1, \hbar_2) = \sum_{m=0}^{+\infty} f_m(t; \hbar_1, \hbar_2) p^m, \tag{29}$$

where

$$u_m(t; \hbar_1, \hbar_2) = \frac{1}{m!} \left. \frac{\partial^m U(t; p, \hbar_1, \hbar_2)}{\partial p^m} \right|_{p=0}, \tag{30}$$

$$v_m(t; \hbar_1, \hbar_2) = \frac{1}{m!} \left. \frac{\partial^m V(t; p, \hbar_1, \hbar_2)}{\partial p^m} \right|_{p=0}, \tag{31}$$

$$f_m(t; \hbar_1, \hbar_2) = \frac{1}{m!} \left. \frac{\partial^m F(t; p, \hbar_1, \hbar_2)}{\partial p^m} \right|_{p=0}. \tag{32}$$

When $p = 1$,

$$U(t; 1, \hbar_1, \hbar_2) = u(t) = \sum_{m=0}^{+\infty} u_m(t; \hbar_1, \hbar_2), \tag{33}$$

$$V(t; 1, \hbar_1, \hbar_2) = v(t) = \sum_{m=0}^{+\infty} v_m(t; \hbar_1, \hbar_2), \tag{34}$$

$$F(t; 1, \hbar_1, \hbar_2) = f(t) = \sum_{m=0}^{+\infty} f_m(t; \hbar_1, \hbar_2), \tag{35}$$

with initial conditions

$$u_0(0; \hbar_1, \hbar_2) = U_0, \qquad v_0(0; \hbar_1, \hbar_2) = V_0, \tag{36}$$

$$u_m(0; \hbar_1, \hbar_2) = v_m(0; \hbar_1, \hbar_2) = 0, \qquad (m \geqslant 1). \tag{37}$$

The solutions $U(t; 1, \hbar_1, \hbar_2)$, $V(t; 1, \hbar_1, \hbar_2)$ and $F(t; 1, \hbar_1, \hbar_2)$ are expressed by $u_m(t; \hbar_1, \hbar_2)$, $v_m(t; \hbar_1, \hbar_2)$ and $f_m(t; \hbar_1, \hbar_2)$, respectively.

As the first step, in order to obtain $u_0(t; \hbar_1, \hbar_2)$, $v_0(t; \hbar_1, \hbar_2)$ and $f_0(t; \hbar_1, \hbar_2)$, we partially differentiate (23)–(25) zero time (i.e. we do not differentiate) with respect to p and set $p = 0$. Equations (23)–(25) become

$$\frac{\partial u_0(t; \hbar_1, \hbar_2)}{\partial t} = 0, \tag{38}$$

$$\frac{\partial v_0(t; \hbar_1, \hbar_2)}{\partial t} = 0, \tag{39}$$

$$f_0^2(t; \hbar_1, \hbar_2) = U_0^2 + V_0^2. \tag{40}$$

From (36), we have

$$u_0(t; \hbar_1, \hbar_2) = U_0, \tag{41}$$

$$v_0(t; \hbar_1, \hbar_2) = V_0, \tag{42}$$

$$f_0(t; \hbar_1, \hbar_2) = \sqrt{U_0^2 + V_0^2}. \tag{43}$$

In the same way, we partially differentiate (23)–(25) m times with respect to p, set $p = 0$ and divide by $m!$, we obtain

$$\frac{\partial u_m(t; \hbar_1, \hbar_2)}{\partial t} = (1 - \hbar_1) \frac{\partial u_{m-1}(t; \hbar_1, \hbar_2)}{\partial t} - \hbar_1 \sum_{k=0}^{m-1} f_k(t; \hbar_1, \hbar_2) u_{m-k-1}(t; \hbar_1, \hbar_2), \tag{44}$$

$$\frac{\partial v_m(t; \hbar_1, \hbar_2)}{\partial t} = (1 - \hbar_1) \frac{\partial v_{m-1}(t; \hbar_1, \hbar_2)}{\partial t}$$
$$- \hbar_1 \sum_{k=0}^{m-1} f_k(t; \hbar_1, \hbar_2) v_{m-k-1}(t; \hbar_1, \hbar_2) - \chi_m \hbar_1, \tag{45}$$

$$f_m(t; \hbar_1, \hbar_2) = \frac{1}{2f_0} \left[-(U_0^2 + V_0^2) \chi_m - \sum_{k=1}^{m-1} f_k(t; \hbar_1, \hbar_2) f_{m-k}(t; \hbar_1, \hbar_2) + (1 - \hbar_2) \right.$$
$$\times \sum_{k=0}^{m-1} f_k(t; \hbar_1, \hbar_2) f_{m-1-k}(t; \hbar_1, \hbar_2) + \hbar_2 \sum_{k=0}^{m-1} \{ u_k(t; \hbar_1, \hbar_2) u_{m-1-k}(t; \hbar_1, \hbar_2)$$
$$\left. + v_k(t; \hbar_1, \hbar_2) v_{m-1-k}(t; \hbar_1, \hbar_2) \} \right], \tag{46}$$

where

$$\chi_m = \begin{cases} 1 & (m = 1), \\ 0 & (m \geqslant 2). \end{cases} \tag{47}$$

Integrating (44) and (45) by t with the initial conditions (37), we obtain

$$u_0(t; \hbar_1, \hbar_2) = U_0, \tag{48}$$

$$u_1(t; \hbar_1, \hbar_2) = -\hbar_1 U_0 \sqrt{U_0^2 + V_0^2} t, \tag{49}$$

$$u_2(t; \hbar_1, \hbar_2) = -(1 - \hbar_1)\hbar_1 U_0 \sqrt{U_0^2 + V_0^2} t + \frac{\hbar_1^2 U_0(U_0^2 + V_0^2)}{2} t^2, \tag{50}$$

$$u_3(t; \hbar_1, \hbar_2) = -(1 - \hbar_1)^2 \hbar_1 U_0 \sqrt{U_0^2 + V_0^2} t$$
$$+ \frac{\hbar_1^2 U_0\{(2 - 2\hbar_1 + \hbar_2)(U_0^2 + V_0^2)^{\frac{3}{2}} + \hbar_2 V_0\}}{2\sqrt{U_0^2 + V_0^2}} t^2 - \frac{\hbar_1^3 U_0(U_0^2 + V_0^2)^{\frac{3}{2}}}{6} t^3, \tag{51}$$

$$\vdots$$

$$v_0(t; \hbar_1, \hbar_2) = V_0, \tag{52}$$

$$v_1(t; \hbar_1, \hbar_2) = -\hbar_1\left(1 + V_0\sqrt{U_0^2 + V_0^2}\right)t, \tag{53}$$

$$v_2(t; \hbar_1, \hbar_2) = -(1 - \hbar_1)\hbar_1\left(1 + V_0\sqrt{U_0^2 + V_0^2}\right)t + \frac{\hbar_1^2 \sqrt{U_0^2 + V_0^2}\left(1 + V_0\sqrt{U_0^2 + V_0^2}\right)}{2} t^2, \tag{54}$$

$$v_3(t; \hbar_1, \hbar_2) = -(1 - \hbar_1)^2 \hbar_1\left(1 + V_0\sqrt{U_0^2 + V_0^2}\right)t + \frac{\hbar_1^2}{2\sqrt{U_0^2 + V_0^2}}$$
$$\times \left[\{-2\hbar_1(U_0^2 + V_0^2) + (2 + \hbar_2)V_0^2\}\left(1 + V_0\sqrt{U_0^2 + V_0^2}\right)\right.$$
$$\left. + U_0^2\{2 + (2 + \hbar_2)V_0\sqrt{U_0^2 + V_0^2}\}\right]t^2 - \frac{\hbar_1^3(U_0^2 + V_0^2)\left(1 + V_0\sqrt{U_0^2 + V_0^2}\right)}{6} t^3,$$
$$\vdots \tag{55}$$

$$f_0(t; \hbar_1, \hbar_2) = \sqrt{U_0^2 + V_0^2}, \tag{56}$$

$$f_1(t; \hbar_1, \hbar_2) = 0, \tag{57}$$

$$f_2(t; \hbar_1, \hbar_2) = -\frac{\hbar_1 \hbar_2\{(U_0^2 + V_0^2)^{\frac{3}{2}} + V_0\}}{\sqrt{U_0^2 + V_0^2}} t, \tag{58}$$

$$f_3(t; \hbar_1, \hbar_2) = \frac{\hbar_1 \hbar_2(-2 + \hbar_1 + \hbar_2)\{(U_0^2 + V_0^2)^{\frac{3}{2}} + V_0\}}{\sqrt{U_0^2 + V_0^2}} t$$
$$+ \frac{\hbar_1^2 \hbar_2\{1 + 2(U_0^2 + V_0^2)^2 + 3V_0\sqrt{U_0^2 + V_0^2}\}}{2\sqrt{U_0^2 + V_0^2}} t^2, \tag{59}$$

$$\vdots$$

4. The power series solution

In the previous section, the solutions of the projectile motion problem with quadratic resistance law can be derived by using the homotopy analysis method. However, those solutions

are so intricate that we cannot obtain the seventh-order approximate solution by means of *MATHEMATICA*. However, we may obtain a power series solution with a recurrence equation [14, 15] from the homotopy analysis solution.

Observing (48)–(59), the structure of the solutions $u_m(t; \hbar_1, \hbar_2)$, $v_m(t; \hbar_1, \hbar_2)$ and $f_m(t; \hbar_1, \hbar_2)$ is found as follows:

$$u_m(t; \hbar_1, \hbar_2) = \sum_{n=0}^{m} a_{m,n} t^n, \tag{60}$$

$$v_m(t; \hbar_1, \hbar_2) = \sum_{n=0}^{m} b_{m,n} t^n, \tag{61}$$

$$f_m(t; \hbar_1, \hbar_2) = \sum_{n=0}^{m} c_{m,n} t^n. \tag{62}$$

Substituting (60)–(62) into (44)–(46), we have

$$\sum_{n=0}^{m} a_{m,n} t^n = (1 - \hbar_1) \sum_{n=0}^{m-1} a_{m-1,n} t^n - \hbar_1 \int_0^t \left\{ \sum_{k=0}^{m-1} \left(\sum_{n=0}^{k} c_{k,n} t^n \sum_{n=0}^{m-k-1} a_{m-k-1,n} t^n \right) \right\} \mathrm{d}t, \tag{63}$$

$$\sum_{n=0}^{m} b_{m,n} t^n = (1 - \hbar_1) \sum_{n=0}^{m-1} b_{m-1,n} t^n$$
$$- \hbar_1 \int_0^t \left\{ \sum_{k=0}^{m-1} \left(\sum_{n=0}^{k} c_{k,n} t^n \sum_{n=0}^{m-k-1} b_{m-k-1,n} t^n \right) \right\} \mathrm{d}t - \chi_m \hbar_1 t, \tag{64}$$

$$\sum_{n=0}^{m} c_{m,n} t^n = \frac{1}{2\sqrt{U_0^2 + V_0^2}} \left[-(U_0^2 + V_0^2) \chi_m - \sum_{k=1}^{m-1} \left(\sum_{n=0}^{k} c_{k,n} t^n \sum_{n=0}^{m-k} c_{m-k,n} t^n \right) \right.$$
$$+ (1 - h) \sum_{k=0}^{m-1} \left(\sum_{n=0}^{k} c_{k,n} t^n \sum_{n=0}^{m-1-k} c_{m-1-k,n} t^n \right)$$
$$\left. + \hbar_1 \sum_{k=0}^{m-1} \left(\sum_{n=0}^{k} a_{k,n} t^n \sum_{n=0}^{m-1-k} a_{m-1-k,n} t^n + \sum_{n=0}^{k} b_{k,n} t^n \sum_{n=0}^{m-1-k} b_{m-1-k,n} t^n \right) \right]. \tag{65}$$

When (63)–(65) holds for an arbitrary t, we have

$$a_{0,0} = U_0, \qquad b_{0,0} = V_0, \qquad c_{0,0} = \sqrt{U_0^2 + V_0^2}, \tag{66}$$

$$a_{m,n} = (1 - \hbar_1) a_{m-1,n} - \frac{\hbar_1}{n} \sum_{k=0}^{m-1} \sum_{i=0}^{n-1} c_{k,i} a_{m-1-k,n-1-i}, \qquad (m \geqslant 1, 1 \leqslant n \leqslant m), \tag{67}$$

$$b_{m,n} = (1 - \hbar_1) b_{m-1,n} - \frac{\hbar_1}{n} \sum_{k=0}^{m-1} \sum_{i=0}^{n-1} c_{k,i} b_{m-1-k,n-1-i} - \chi_{m,n} \hbar_1, \qquad (m \geqslant 1, 1 \leqslant n \leqslant m), \tag{68}$$

$$c_{m,n} = \frac{1}{2\sqrt{U_0^2 + V_0^2}} \left[-\sum_{k=1}^{m-1}\sum_{i=0}^{n} c_{k,i} c_{m-k,n-i} + (1 - \hbar_2)\sum_{k=0}^{m-1}\sum_{i=0}^{n} c_{k,i} c_{m-1-k,n-i} \right.$$

$$\left. +\hbar_2 \sum_{k=0}^{m-1}\sum_{i=0}^{n} (a_{k,i} a_{m-1-k,n-i} + b_{k,i} b_{m-1-k,n-i}) \right],$$

$$(m \geqslant 1, 1 \leqslant n \leqslant m - 1), \tag{69}$$

where $\chi_{1,1} = 1$, $\chi_{m,n} = 0$ $(m \neq 1 \vee n \neq 1)$, $a_{m,n} = b_{m,n} = 0$ $(m < n)$, $c_{m,n} = 0$ $(m \leqslant n)$.

Now, we obtain ultimate solutions

$$u(t) = \sum_{m=0}^{+\infty}\sum_{n=0}^{m} a_{m,n} t^n, \tag{70}$$

$$v(t) = \sum_{m=0}^{+\infty}\sum_{n=0}^{m} b_{m,n} t^n, \tag{71}$$

$$f(t) = \sum_{m=0}^{+\infty}\sum_{n=0}^{m} c_{m,n} t^n. \tag{72}$$

As a consequence, we have the non-dimensional positions $x(t)$ and $y(t)$ as follows:

$$x(t) = \sum_{m=0}^{+\infty}\sum_{n=0}^{m} \frac{1}{n+1} a_{m,n} t^{n+1}, \tag{73}$$

$$y(t) = \sum_{m=0}^{+\infty}\sum_{n=0}^{m} \frac{1}{n+1} b_{m,n} t^{n+1}, \tag{74}$$

where $x(0) = y(0) = 0$.

5. Optimization method of the homotopy parameters and discussions

Liao [7] shows the guideline that the convergence radius increases as the homotopy parameters decrease. Abbasbandy [16, 17] investigated the error of the homotopy analysis solution for the homotopy parameter by comparing with the exact solution. In this section, we show the optimization method of the homotopy parameters $\hbar_1, \hbar_2$ for the order of approximation N. The homotopy parameter is an arbitrary constant when N is infinite; however, the optimum value of homotopy parameter should be found under the finite number of N. This method can be applied to the problem without the exact solution. The Nth-order approximate solutions of (70)–(72) are defined as follows:

$$\tilde{u}_N(t; \hbar_1, \hbar_2) = \sum_{m=0}^{N}\sum_{n=0}^{m} a_{m,n} t^n, \tag{75}$$

$$\tilde{v}_N(t; \hbar_1, \hbar_2) = \sum_{m=0}^{N}\sum_{n=0}^{m} b_{m,n} t^n, \tag{76}$$

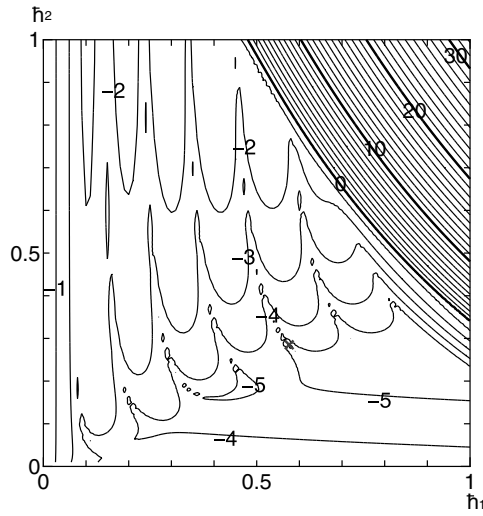$$\tilde{f}_N(t; \hbar_1, \hbar_2) = \sum_{m=0}^{N}\sum_{n=0}^{m} c_{m,n} t^n. \tag{77}$$

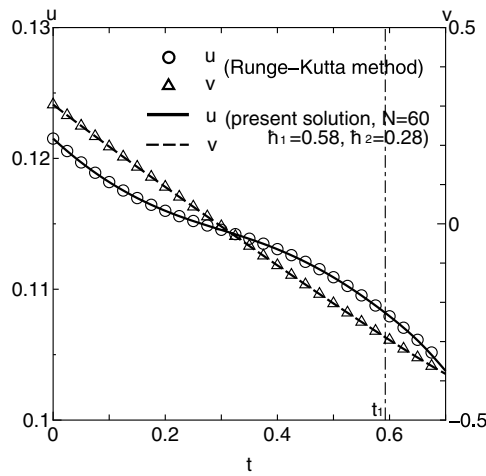**Figure 1.** Contours of $\log_{10} \varepsilon_{60}(\hbar_1, \hbar_2)$.

Figure 2. Variations of $u, v(\hat{U}_0 = 2 \text{ m s}^{-1}, \hat{V}_0 = 5 \text{ m s}^{-1})$.

The initial conditions are

$$\hat{U}_0 = 2 \text{ m s}^{-1}, \qquad \hat{V}_0 = 5 \text{ m s}^{-1},$$

$$U_0 \approx 0.122, \qquad V_0 \approx 0.304,$$

$$v_t = \sqrt{\frac{g}{\alpha}} = \sqrt{\frac{2Mg}{\rho \pi a^2 C_D}} = \sqrt{\frac{2 \times 0.27 \times 9.8}{1.2 \times \pi \times 0.105^2 \times 0.47}} \approx 16.46 \text{ m s}^{-1},$$

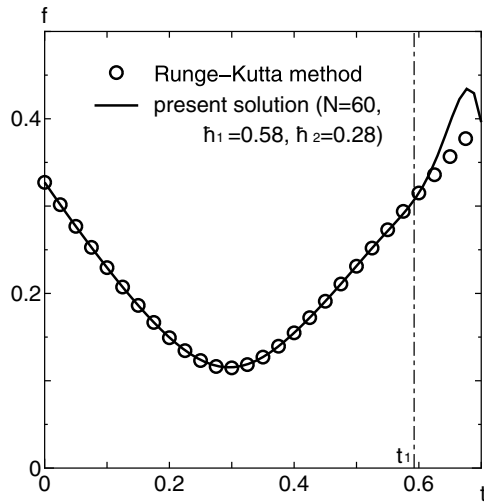(78)

where a volleyball's dimensions are used in this paper.

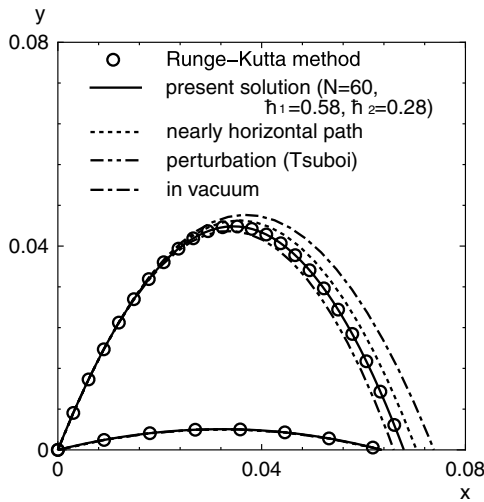**Figure 3.** Variation of f ($\hat{U}_0 = 2$ m s^{-1}, $\hat{V}_0 = 5$ m s^{-1}).

Figure 4. Comparison of orbits between nearly horizontal path, perturbation solution (Tsuboi), Runge–Kutta solution and the present solution.

We consider a residual of the Nth-order approximate solutions for (15), (16) from $t = 0$ to t_1. The residual is expressed as follows:

$$\varepsilon_N(\hbar_1, \hbar_2) = \left[\left\{ \int_0^{t_1} \left(\frac{\partial \tilde{u}_N(t; \hbar_1, \hbar_2)}{\partial t} + \tilde{f}_N t; \hbar_1, \hbar_2) \tilde{u}_N(t; \hbar_1, \hbar_2) \right) dt \right\}^2 \right.$$

$$\left. + \left\{ \int_0^{t_1} \left(\frac{\partial \tilde{v}_N(t; \hbar_1, \hbar_2)}{\partial t} + \tilde{f}_N(t; \hbar_1, \hbar_2) \tilde{v}_N(t; \hbar_1, \hbar_2) + 1 \right) dt \right\}^2 \right]^{\frac{1}{2}} \tag{79}$$

where $t_1 = 0.5924$ is the non-dimensional time when the orbits cross the x-axis (landing). As the present solution approaches the exact solution, the value of $\varepsilon_N(\hbar_1, \hbar_2)$ approaches zero. Figure 1 shows the contour lines of $\log_{10} \varepsilon_N(\hbar_1, \hbar_2)$ when $N = 60$. $\hbar_1$ is in ordinate
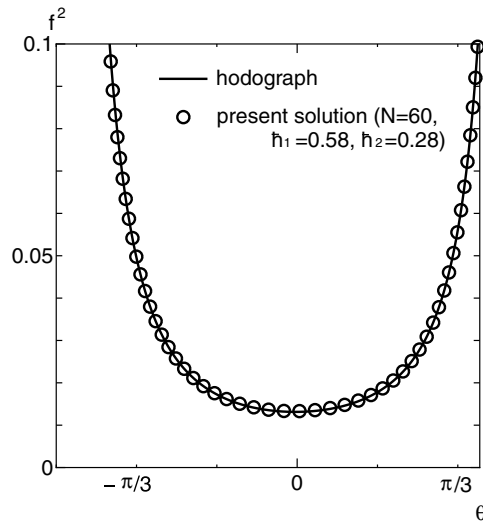
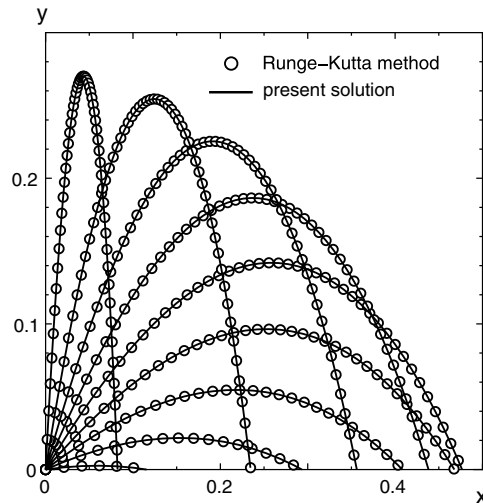**Figure 5.** Comparison between the hodograph solution and the present solution.

Figure 6. Projectile pathes for various angles of projection ($\sqrt{\hat{U}_0^2 + \hat{V}_0^2} = 14$ m s^{-1}).

and $\hbar_2$ is in abscissa. The contour interval is 1.0. A minimum point of $\log_{10} \varepsilon_{60}(\hbar_1, \hbar_2)$ is $\hbar_1 = 0.58, \hbar_2 = 0.28$ in figure 1. Those values are optimal values of $\hbar_1, \hbar_2$ for the order $N = 60$.

Figures 2 and 3 show variations of $\tilde{u}_{60}(t; \hbar_1, \hbar_2), \tilde{v}_{60}(t; \hbar_1, \hbar_2)$ and variation of $\tilde{f}_{60}(t; \hbar_1, \hbar_2)$ when $\hbar_1 = 0.58, \hbar_2 = 0.28$. Those solutions are compared with the numerical solutions of the Runge–Kutta method. The present 60th-order solutions are in good agreement with the numerical solutions in the region of $0 \leqslant t \leqslant t_1$. Figure 4 illustrates the projectile paths. In figure 4, orbits of the nearly horizontal path, the perturbation method (Tsuboi), and the present solution are compared with the numerical result of the Runge–Kutta method. When the angle of projection is small ($\hat{U}_0 = 6$ m s^{-1}, $\hat{V}_0 = 1.5$ m s^{-1}, $\theta_0 \approx 14$ degrees), those orbits coincide with the orbit of the numerical solution, where $N = 10, \hbar_1 = 0.97, \hbar_2 = 0.28$.
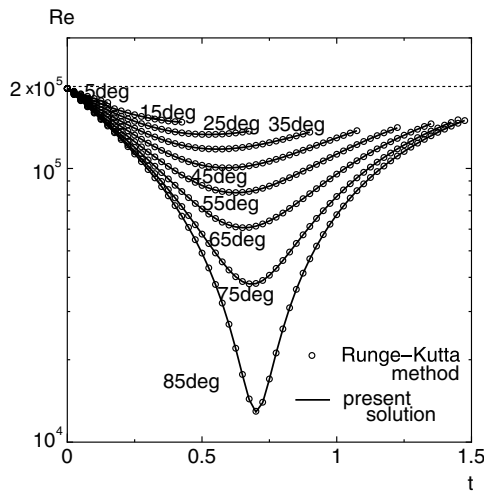
Figure 7. Variations of Reynolds number during motion ($\sqrt{\hat{U}_0^2 + \hat{V}_0^2} = 14$ m s^{-1}).

Table 1. The values of $t_1, N, \hbar_1, \hbar_2$ for various angles of projection.

Angle of projection (deg)	t_1	N	$\hbar_1$	$\hbar_2$
5	0.1453	10	0.90	0.73
15	0.4162	20	0.89	0.63
25	0.6600	30	0.76	0.58
35	0.8760	30	0.83	0.39
45	1.0631	30	0.57	0.33
55	1.2193	40	0.31	0.28
65	1.3418	70	0.46	0.38
75	1.4270	100	0.30	0.30
85	1.4710	120	0.27	0.22

When the angle of projection is large ($\hat{U}_0 = 2$ m s^{-1}, $\hat{V}_0 = 5$ m s^{-1}, $\theta_0 \approx 68$ degrees), orbits of the nearly horizontal path and the perturbation method (Tsuboi) disagree with the orbit of the numerical solution. In contrast, the orbit of the present 60th-order approximate solution agrees with the numerical solution. Figure 5 shows a comparison between the hodograph solution and the present solution in the above case in which the angle of projection is large. The present 60th-order approximate solution also agrees with the hodograph solution in the θ coordinate.

In figure 6, the present solution is compared with the Runge–Kutta solution for various angles of projection $\left(\sqrt{\hat{U}_0^2 + \hat{V}_0^2} = 14 \text{ m s}^{-1}\right)$. It can be known that the present solution is in agreement with the numerical solution. The values of $\hbar_1, \hbar_2$ are determined using a minimum value of (79) and are shown in table 1 with t_1 and N. Table 1 shows that the order of approximation N is small and $\hbar_1, \hbar_2$ are large when the differential equation has weak nonlinearity (i.e. small angle of projection), and that N increases and $\hbar_1, \hbar_2$ decrease as nonlinearity increases (i.e. the large angle of projection). Figure 7 shows variation of the Reynolds number in each case during motion. The end points of lines indicate t_1. It is found that these results are within the range $1 \times 10^3 < Re < 2 \times 10^5$ that C_D is considered as constant and that the initial velocity $\sqrt{\hat{U}_0^2 + \hat{V}_0^2}$ is almost the maximum value under the quadratic resistance

law. It is predicted that the present solution is valid when the dimensionless initial velocities U_0 and V_0 is smaller than the present case, however, the solution may be invalid for a much larger dimensionless initial velocity, because the present solution is a polynomial expression as shown in (73) and (74).

6. Conclusion

An analytic solution of the problem of two-dimensional projectile motion with quadratic resistance law for a large angle of projection is obtained using the homotopy analysis method. The solution is derived by means of constructing the zeroth-order deformation equations for not only governing differential equations, but also an algebraic equation of a velocity vector. The solution is expressed as simple power series. A residual obtained by substituting the power series solution into the governing equation is introduced to optimize the value of the homotopy parameters $\hbar_1, \hbar_2$. The optimum values of $\hbar_1, \hbar_2$ for the order of approximation N are determined successfully. The present solution has sufficient accuracy because the solution agrees with the hodograph solution and the Runge–Kutta solution.

References

[1] White F M 1991 *Viscous Fluid Flow* 2nd edn (New York: McGraw-Hill) pp 177, 182, 183
[2] Lamb H 1923 *Dynamics* (London: Cambridge University Press) p 294
[3] Parker G W 1977 Projectile motion with air resistance quadratic in the speed *Am. J. Phys.* **45** 606
[4] Tsuboi K 1996 On the optimum angle of takeoff in long jump *Trans. Japan Soc. Ind. Appl. Math.* **6** 393
[5] Apostolatos T A 2002 Hodograph: a useful geometrical tool for solving some difficult problems in dynamics *Am. J. Phys.* **71** 261
[6] Goto K 1983 *Rikigaku-ensyu* (Tokyo: Kyoritsu Shuppan) pp 11, 47
[7] Liao S J 2004 *Beyond Perturbation* (Boca Raton: Chapman and Hall)
[8] Allan F M 2007 Derivation of the Adomian decomposition method using the homotopy analysis method *Appl. Math. Comput.* **190** 6
[9] Liao S J 1992 A second-order approximate analytical solution of a simple pendulum by the process analysis method *J. Appl. Mech.* **59** 970
[10] Liao S J 1997 A kind of approximate solution technique which does not depend upon small parameters: II. An application in fluid mechanics *Int. J. Non-linear Mech.* **32** 815
[11] Liao S J 2006 Series solutions of unsteady boundary-layer flows over a stretching flat plate *Stud. Appl. Mech.* **117** 239
[12] Xu H and Liao S J 2005 Series solutions of unsteady magnetohydrodynamic flows of non-Newtonian fluids caused by an impulsivery stretching plate *J. Non-Newton. Fluid Mech.* **129** 46
[13] Liao S J 2002 An analytic approximation of the drag coefficient for the viscous flow past a sphere *Int. J. Non-linear Mech.* **37** 1
[14] Hayat T and Sajid M 2007 On analytic solution for thin film flow of a forth grade fuluid down a vertical cylinder *Phys. Lett.* A **361** 316
[15] Sajid M, Hayat M and Asghar S 2006 Comparison between the HAM and HPM solutions of thin film flows of non-Newtonian fluids on a moving belt *Nonlinear Dyn.* DOI:10.1007/S11071-006-9140-y
[16] Abbasbandy S 2006 The application of homotopy analysis method to nonlinear equations arising in heat transfer *Phys. Lett.* A **360** 109
[17] Abbasbandy S 2007 The application of homotopy analysis method to solve a generalized Hirota–Satsuma coupled KdV equation *Phys. Lett.* A **361** 478